Pulsed Interference Cancellation Based on Unused Spatial Dimensions and Lattice Signal Sets

Khodr A. Saaifan and Werner Henkel
Transmission Systems Group (TrSyS)
Jacobs University Bremen
Bremen 28759, Germany
{k.saaifan, w.henkel}@jacobs-university.de

***Abstract*—The inlay approach of an L-band Digital Aeronautical Communications System (L-DACS) is exposed to severe interference from the adjacent channels of distance measuring equipment (DME). Here, we propose two schemes to mitigate DME interference and subsequently enable transmission in the spectral gaps of the DME channels. The first scheme is suitable when the channel remains the same for a long time and it is making use of the unused spatial dimensions for a singular value decomposition (SVD) approach. In the second scheme, we develop an interleaved lattice code with subcarrier clipping to reduce the impacts of DME in frequency domain. The simulation results indicate that the proposed schemes can guarantee reliable communication in the presence of strong DME interference. Moreover, the simulation in a realistic interference scenario shows that the proposed approaches provide a good performace in fading channels.**

***Index Terms*—OFDM, DME, SVD, lattice signal set**

I. Introduction

L-DACS1 is a broadband candidate for a future L-band digital aeronautical communications system. Such a system has been proposed by the German Aerospace Center (DLR) [1]. The physical layer of the L-DACS1 system employing Orthogonal Frequency-Division Multiplexing (OFDM) as modulation scheme and Frequency-Division Duplex (FDD) for separating forward (FL) and reverse link (RL).

In this paper, we focus on non-stationary interference originating from nearby DME channels to an L-band digital aeronautical communications system (L-DACS1). The aeronautical part of the L-band is mainly used by DME or tactical air navigation systems (TACAN). These systems are used for determining the slant range between an airborne and a ground station. For an efficient use of bandwidth in the L-band, the L-DACS1 system is developed as an inlay system between two adjacent DME channels. The inlay approach makes L-DACS1 subject to strong interference originating from existing L-band systems. For reducing out-of-band radiation of the OFDM signal causing interference towards the licensed system, powerful techniques have been proposed in [2]. To mitigate the impact of DME signals, clipping and pulse blanking have been developed and applied to L-DACS1 [3]. In addition, an erasure-based convolutional decoding strategy has been investigated in [4] to mitigate the impact of DME interference. In [5], We introduced lattice signal sets with subcarrier clipping during the flight mode of the aircraft (en-route scenario) to reduce the impact of DME signals in frequency domain.

Here, we consider a parking scenario of an aircraft. This scenario is characterized by a Rayleigh fading channel with strong DME interference. Since the channel of this scenario stays the same for a long time, we propose to use the unused spatial dimensions for an SVD approach to extract a reference signal of the interference. For efficient DME cancellation, we propose to combine an SVD approach with lattice signal sets, which can significantly reduce the impact of interference from the impaired subcarriers.

This paper is organized as follows. Section II briefly describes the system model and background. In Section III, we introduce the proposed DME mitigation techniques for L-DACS1. Finally, simulation results and concluding remarks are presented in sections IV and V, respectively.

II. System Model and Background

A. System Model

The physical layer of L-DACS1 is based on OFDM modulation and designed to operate in the aeronautical L-band (960 -1164 MHz). A detailed physical layer description including all relevant OFDM parameters is given in [3]. According to these parameters, a bandwidth of 500 kHz is considered to be available for each B-AMC forward (FL) or reverse link (RL) channel, with 48 subcarriers used for data transmission. An FFT of length $N = 64$ is used with 8 guard subcarriers on the left and the right side of the spectrum for filtering purposes. The guard interval (cyclic prefix) consumes 20 % of the overall OFDM symbol duration, which is relatively long, but not untypical for wireless systems. One half of the guard interval is used as conventional guard time to avoid inter-symbol interference between successive OFDM symbols. The other half is used for transmit-pulse shaping in order to decrease out-of-band radiation.

B. Channel Models for Different Flight Modes

The different conditions during a flight of an aircraft lead to different channel scenarios. These scenarios are characterized by the type of fading, the Doppler frequency f_d, and the delay spread τ, where the Doppler and the delay power spectra represent the diffusely scattered multipath components. As representative scenarios, an en-route, a take-off/landing, and a parking scenario are considered.

TABLE I
CHANNEL MODEL PARAMETERS FOR DIFFERENT FLIGHT SCENARIO [1]

Scenario	fading	delay	Doppler
en-route	Ricean (Rice factor $K_R = 15$ dB)	direct + 2 delay paths	Gaussian (f_D = 1.25 kHz)
take-off/landing	Ricean (Rice factor $K_R = 10$ dB)	exponential ($\tau = 20\mu$s)	Jakes (f_D = 512 Hz)
parking	Rayleigh	exponential ($\tau = 3$ μs)	Jakes (f_D = 18 Hz)

C. DME/TACAN Interfering Signal

The basic DME/TACAN signal consists of two Gaussian-shaped pulses with an inter-pulse interval Δt of either 12 μs (X-mode) or 36 μs (Y-mode). For us, only the DME/TACAN signal in X-mode is of interest, which can be expressed as [6]

$$d(t) = e^{-\frac{\alpha}{2}t^2} + e^{-\frac{\alpha}{2}(t-\Delta t)^2} \; . \tag{1}$$

The parameter $\alpha = 4.5 \cdot 10^{11}$ s^{-2} is set such that the pulse width is 3.5 μs. The interference signal at the OFDM receiver can be considered as the superposition of N_{dme} contributing transmitters from DME stations operating in the same or different DME channels. The resulting interference signal can be expressed as [3]

$$i(t) = \sum_{i=1}^{N_{\mathrm{dme}}} \sum_{p=1}^{N_i} A_i d(t - t_{i,p}) e^{j2\pi f_{c,i} t + j\phi_i} \; , \tag{2}$$

where N_{dme} is the number of DME stations, N_i, $i = 1, \ldots, N_{\mathrm{dme}}$ represents the number of pulse pairs in the considered time interval for the i^{th} DME station, A_i denotes the peak amplitude of the i^{th} DME signal, $t_{i,p}$, $p = 1, \ldots, N_i$ are the starting times of the non-overlapped N_i pulse pairs of the i^{th} DME station, and ϕ_i represents the phase of the i^{th} DME signal, which is uniformly distributed over $(-\pi, \pi]$. In order to simulate the impact of DME/TACAN ground stations on the L-DACS1, the simulation model suggested in [1] has been adopted to build our own simulator.

To analyze the effect of interference for different flight phases, worst-case scenarios are considered [1]. For a parking scenario, the interference power originating from the close-by stations is considered, only. In this case, one strong interference is simulated at $+0.5$ MHz offsets to the L-DACS1 center frequency with a power of -22.4 dBm. For an en-route scenario, there are two interferers with a power of up to -74 dBm at $+0.5$ MHz and one strong interferer is present at -0.5 MHz with a power of -67.9 dBm. The pulse rate of each interferer is 3600 pulse pairs per second (ppps).

III. INTERFERENCE CANCELLATION

A. Lattice Signal Sets with Subcarrier Clipping

In [5], we introduced a more general interference mitigation method, that can be implemented for all airborne flight scenarios. The DME spectrum mitigation technique is directed towards lattice signal sets realizing signal space diversity [7]. This type of diversity is widely used for designing a high-rate full-diversity space-time (ST) [8], [9] and space-time-frequency (STF) code [10] in MIMO systems.

For L-DACS1, a vector $\mathbf{S}$ of N_s QAM symbols for the used subcarriers is subdivided into P parallel sub-blocks, where $P = N_s/M$ and M is the dimension of the lattice signal set. The sub-blocks are encoded simultaneously into lattice code vectors $\mathbf{X}_p = \mathbf{G}_M \mathbf{S}_p$, $p = 1, \ldots, P$, where $\mathbf{G}_M$ is the fully diverse unitary matrix defined in [9]. The code vectors from sub-blocks are concatenated and interleaved to generate a lattice codeword $\mathbf{X}$ of size $N_s \times 1$, which is forwarded to the N-point IFFT block. At the receiver after FFT operation, the received signal components for used subcarriers can be expressed as

$$Y[k] = H[k]X[k] + Z[k] + I[k] \; , \quad k = 8, 9, \cdots, 55 \; , \tag{3}$$

where $H[k]$ is the frequency response of the channel, $Z[k]$ is the AWGN sample, and $I[k]$ is the DME signal contribution. The idea behind employing lattice signal sets is to cancel out the interference in frequency domain, where the interference spectrum is almost known to be hitting the outer subcarriers of L-DACS1. The idea of using interleaving is to spread the received DME interference over all used subcarriers before applying the lattice decoder [11], which subsequently averages out the effect over all used subcarriers. As a cancellation scheme, we suggested a simple clipping technique to clip the impaired subcarriers (outer subcarriers) in order to improve the signal-to-interference-and-noise ratio (SINR) after the lattice decoding. The amplitudes of the received signals at the outer subcarriers (severely impaired by DME interference) are reduced to a certain thresholds $T^c[k]$ when their amplitude exceeds $T^c[k]$. The clipping operation yields the clipped received signal as follows:

$$Y^c[K] = \begin{cases} Y[k] & \text{if } |Y[k]| \leq T^c[k] \\ T^c[k]e^{j\arg(Y[k])} & \text{otherwise} \end{cases} . \quad (4)$$

It is clear that not only the interference signal but also the noise and the desired signal are affected by clipping. In [5], the clipping impact is kept at an acceptable level by optimizing the clipping thresholds $T^c[k]$ as a trade-off between the achieved reduction of interference power and the impact on the desired signal.

In [5], employing an interleaved lattice signal set with clipping as an interference mitigation scheme is examined for an en-route scenario. Hereto, we consider a worse interference condition which occurs during the parking scenario. In this scenario, we have one strong interference at $+0.5$ MHz from the L-DACS1 center frequency with a power of -22.4 dBm. In Fig. 1, we show the interference spectrum (resulting from the DME signal and noise) before and after subcarrier clipping. The clipping operations are applied to the last twenty subcarriers. As we can see from this figure, the impact of interference is reduced by 44 dB. The remaining gap (6 dB) between the interference power after subcarrier clipping and the interference-free case can be justified as a distortion that is induced by the clipping operation.

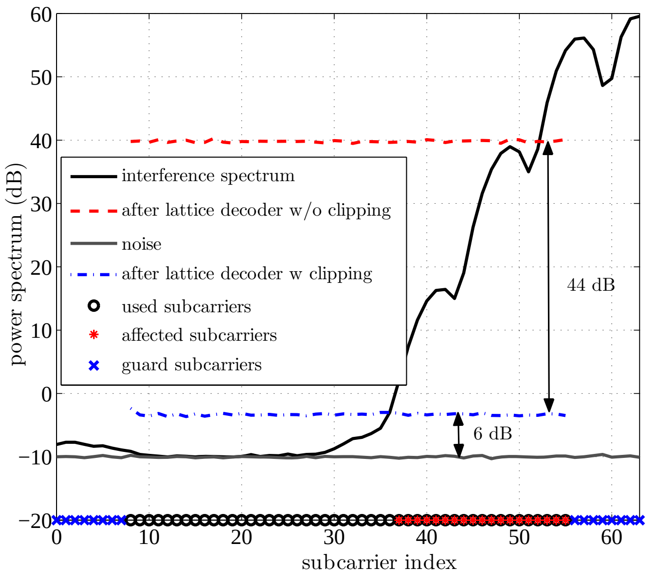

Fig. 1. Spectrum of interfering signal before and after lattice decoding at an SNR of 10 dB

B. Spatial Redundancy

In the parking scenario, the aircraft is on the ground and moving at a very low speed close to the terminal or is parked at the terminal. The channel state information (CSI) remains constant over the L-DACS1 frame (54 OFDM symbols) and consequently, the CSI can be assumed to be available at the transmitter (via a feedback channel). Here, we investigated SVD redundancy [12] to cancel the DME spectrum. For simplicity, in this paper we only consider a 2×2 MIMO-OFDM system with N subcarriers. We actually make use of OFDM for every spatial channel, meaning a channel matrix $\mathbf{H}[k]$ for every k^{th} subcarrier which can be expressed as

$$\mathbf{H}[k] = \begin{bmatrix} H_{11}[k] & H_{12}[k] \\ H_{21}[k] & H_{22}[k] \end{bmatrix} . \quad (5)$$

$H_{n_r n_t}[k]$ is the channel frequency response between the n_t^{th} transmit antenna and the n_r^{th} receive antenna. $H_{n_r n_t}[k]$ is given by

$$H_{n_r n_t}[k] = \mathbf{W}_N[k]\mathbf{h}_{n_r n_t} , \quad k = 0, 1, \cdots, N-1 . \quad (6)$$

$\mathbf{h}_{n_r n_t} = [h_{n_r n_t}[0], h_{n_r n_t}[1], \cdots, h_{n_r n_t}[L-1]]^T$ contains the time response of an L taps channel model, and $\mathbf{W}_N[k] = [1, e^{-j2\pi k/N}, \cdots, e^{-j2\pi k(L-1)/N}]$ contains a row of the DFT matrix. A well-known tool in wireless and wireline MIMO communication is the singular value decomposition (SVD) which diagonalizes a channel matrix $\mathbf{H}[k]$ in the form

$$\mathbf{H}[k] = \mathbf{V}[k]\mathbf{D}[k]\mathbf{U}[k]^H . \quad (7)$$

When a transmit vector $\mathbf{S}[k] = [S_1[k] \;\; S_2[k]]^T$, where $S_{n_t}[k]$ is a transmitted symbol at the k^{th} subcarrier from transmit-antenna n_t, is preprocessed by $\mathbf{U}[k]$, and the receiver provides a post-processing $\mathbf{V}[k]^H$, then only the diagonal matrix $\mathbf{D}[k]$ remains, which represents the independent spatial channels. The pre- and postprocessing matrices are unitary. Typically, in wireless channels, there are dominant eigenchannels and also very poor ones, that are often not used at all. By allocating zero(s) to the weakest eigenchannel(s), the transmitted signal can be expressed as

$$\mathbf{X}[k] = \begin{bmatrix} X_1[k] \\ X_2[k] \end{bmatrix} = \mathbf{U}[k] \begin{bmatrix} S_1[k] \\ 0 \end{bmatrix} . \quad (8)$$

At the receiver front-end, the received signal consists of the desired OFDM signal, AWGN component, and DME interference contribution. After the FFT operation, the received signal on the k^{th} subcarrier is given by

$$\begin{bmatrix} Y_1[k] \\ Y_2[k] \end{bmatrix} = \mathbf{H}[k] \begin{bmatrix} X_1[k] \\ X_2[k] \end{bmatrix} + \begin{bmatrix} Z_1[k] \\ Z_2[k] \end{bmatrix} + \begin{bmatrix} I_1[k] \\ I_2[k] \end{bmatrix} , \quad (9)$$

where Z_{n_r}, $n_r = 1, 2$ are the AWGN and I_{n_r}, $n_r = 1, 2$ are the FFT counterparts of the received DME signal $i_{n_r}(t) = \alpha_{n_r}(t) * i(t)$, where $\alpha_{n_r}(t)$ is the interference channel impulse response to the n_r^{th} receive antenna. After post-processing by matrix $\mathbf{V}[k]^H$, we obtain

$$\begin{bmatrix} \tilde{Y}_1[k] \\ \tilde{Y}_2[k] \end{bmatrix} = \begin{bmatrix} D_1[k]S_1[k] \\ 0 \end{bmatrix} + \begin{bmatrix} \tilde{Z}_1[k] \\ \tilde{Z}_2[k] \end{bmatrix} + \begin{bmatrix} \tilde{I}_1[k] \\ \tilde{I}_2[k] \end{bmatrix} . \quad (10)$$

We observe that, using the proposed spatial redundancy, we can supply the receiver with a reference replica of the received DME interference. Therefore, this reference signal can be used to cancel the effect of the DME spectrum received at the first antenna.

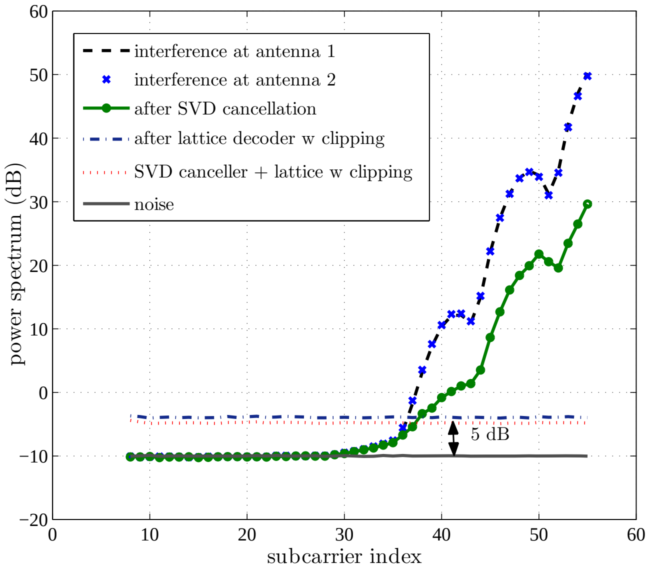

Fig. 2. Spectrum of interfering signal after the proposed SVD-based canceller at an SNR of 10 dB

Figure 2 depicts the power spectrum of the received interfering signals (DME signal and noise) before and after the SVD-based cancellation. The interfering signals are randomly generated for 1500 OFDM frames and the resulting spectra are averaged over all trials. We can see that the impact of interference at high subcarriers is reduced by 22 dB. Since the lattice signal set with clipping offers a better interference power reduction, concatenating the SVD cancellation approach with lattice signal set is also simulated and depicted in Fig. 2. As it can be seen, by employing both cancellation techniques, the interference power is reduced by 45 dB. We can see only 1 dB gap between the two cancellation schemes, but the concatenating approach appears to be more efficient, since it uses the strongest eigenchannel for data transmission.

IV. Simulation Results

The performance of the L-DACS1 system is simulated and compared in terms of the bit-error ratio (BER) with a lattice code based canceller and an SVD-based approach. The data symbols are QPSK modulated with a (133,171) convolutional code (CC) of rate 1/2. To improve the correcting capability of the CC, a random interleaver for all encoded bits within an OFDM frame is introduced as discussed in [4]. A lattice signal set of dimension $M = 24$ is considered [5].

Figure 3 shows the BER performance for the parking and en-route channel models. In the absence of interference, the performance over the en-route channel is close to the performance over an AWGN channel (not shown in Figure 3) due to the strong line-of-sight (LOS) component. In the parking scenario, the performance is similar to the performance of a frequency-selective Rayleigh fading channel. In the presence of interference, we can see from this figure that the performance improvement after employing a lattice signal set with clipping to combat the DME signal. At a BER of 10^{-3}, we have a gap of 1 dB and 6 dB between the lattice-based technique and interference-free case in the en-route and parking channel model, respectively. In this figure, we can see as well the performance improvement introduced by employing the SVD approach in the parking scenario. The proposed SVD-based cancellation approach uses the strongest eigenchannel of a MIMO system, which improves the system performance over a Rayleigh fading channel.

V. Conclusion

In this work, DME interference suppression for OFDM-based inlay systems is considered. Using a lattice signal set with an SVD approach of a MIMO system, the DME mitigation problem is moved into the frequency domain, where a simple clipping method has been introduced. It has been confirmed by means of simulation that the proposed clipping method is capable of considerably reducing the impact of DME interference and provides a good performance over fading channels. Furthermore,

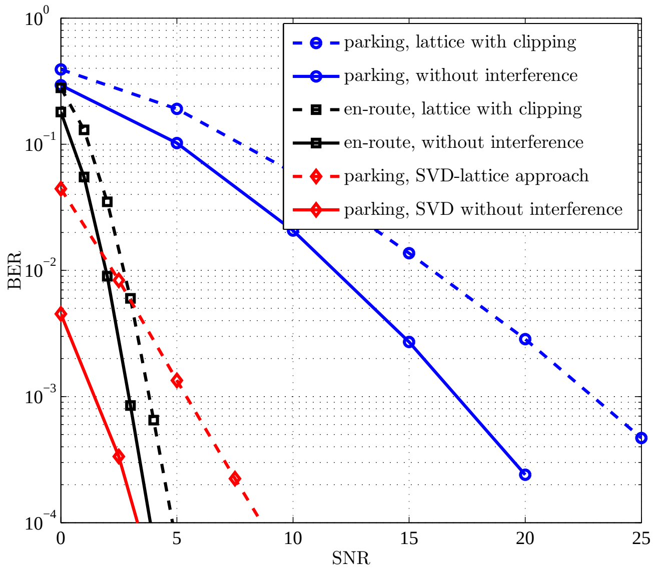

Fig. 3. BER performance over the parking and en-route channel model

the simulation in a realistic interference scenario has shown that the proposed approach provides a reasonable BER performance.

Acknowledgment

This work is funded by the German National Science Foundation (Deutsche Forschungsgemeinschaft, DFG).

References

[1] S. Brandes, S. Gligorevic, M. Ehammer, T. Grüpl, C. H. Rokitansky, R. Dittrich, M. Schnell, and C. Rihacek, "Expected B-AMC System Performance," Tech. report, DLR, 2007.

[2] S. Brandes, I. Cosovic, and M. Schnell, "Reduction of Out-of-Band Radiation in OFDM Systems by Insertion of Cancellation Carriers," *IEEE Communications Letters*, vol. 10, pp. 420–422, June 2006.

[3] S. Brandes, *Suppression of Mutual Interference in OFDM Based Overlay Systems*, Ph.D. thesis, Karlsruhe Institute of Technology, 2009.

[4] M. Schnell, S. Brandes, S. Gligorevic, M. Walter, C. Rihacek, M. Sajatovic, and B. Haindl, "Interference Mitigation for Broadband L-DACS," in *27th Digital Avionics Systems Conference (DASC)*, St. Paul, MN, USA, October 2008.

[5] K. A. Saaifan and W. Henkel, "Lattice Signal Sets to Combat Pulsed Interference from Aeronautical Signals," in *IEEE International Conference on Communications (ICC)*, Japan, June 2011.

[6] G. X. Gao, "DME/TACAN Interference and its Mitigation in L5/E5 Bands," in *On Global Navigation Satellite Systems Conference 2007*, Fort Worth, Texas, September 2007.

[7] J. Boutros and E. Viterbo, "Signal Space Diversity: A Power and Bandwidth Efficient Diversity Technique for the Rayleigh Fading Channel," *IEEE Transactions on Information Theory*, vol. 44, pp. 1453–1467, July 1998.

[8] M. O. Damen, K. A. Meraim, and J. C. Belfiore, "Diagonal Algebraic Space-Time Block Codes," *IEEE Transactions on Information Theory*, vol. 48, pp. 628–636, March 2002.

[9] H. ElGamal and M. O. Damen, "Universal Space-Time Coding," *IEEE Transactions on Information Theory*, vol. 49, pp. 1097–1119, May 2003.

[10] W. Zhang, X.-G. Xia, and P. C. Ching, "High-Rate Full-Diversity Space-Time-Frequency Codes for Broadband MIMO Block Fading Channels," *IEEE Transactions on Communications*, vol. 55, pp. 25–34, January 2007.

[11] E. Viterbo and E. Biglieri, "A Universal Decoding Algorithm for Lattice Codes," *GRETSI Symposium on Signal and Image Processing*, pp. 611–614, September 1993.

[12] W. Henkel, "RS codes, OFDM, and MIMO," in *15th International OFDM-Workshop 2010*, Hamburg, Germany, August 2010.